Pure Appl. Chem., Vol. 73, No. 9, pp. 1477–1485, 2001.

Rational design and synthesis of homochiral azole antifungal agents*

Maurizio Botta†, Federico Corelli, Fabrizio Manetti, Claudia Mugnaini, and Andrea Tafi

Dipartimento Farmaco Chimico Tecnologico, Università degli Studi di Siena, Via A. Moro, 53100 Siena, Italy

Abstract: The first synthesis of both enantiomers of the antifungal drug bifonazole (**1a**) and related imidazole compounds **1i** and **5b,c** is described, starting from enantiomerically pure or enriched amines **6a–d**. Construction of the imidazole ring on amines **6a–d** was performed in a straightforward manner affording the final compounds in good overall yield and with very high enantiomeric purity, as determined by enantioselective HPLC. Biological evaluation *in vitro* of the single enantiomers of **1a,i** and **5b,c** against different strains of *Candida albicans* did not show any enantioselectivity. Finally, the pseudoreceptor modeling technique was applied to generate a model able to explain and predict the inhibitory activity of azole compounds against *C. albicans* $P450_{14DM}$.

INTRODUCTION

Cytochromes P-450 constitute a suprafamily of enzymes that catalyze the oxidation of a large range of biological substrates. They bind dioxygen to the iron atom of their protoporphyrin moiety and through a stepwise cleavage of the O_2 double bond incorporate one oxygen atom into nonactivated C–H bonds. In extension to oxygen insertion reactions, some enzymes of the P-450 suprafamily can catalyze a sequence of reactions leading to a C–C bond cleavage. Cytochrome P-450-dependent lanosterol 14α-demethylase ($P450_{14DM}$), in particular, catalyzes the first step of the conversion of lanosterol to cholesterol (mammals) or ergosterol (fungi), that are important constituents of the cell membrane, by causing the removal of the 14α-methyl group of substrate to give the Δ14-15-desaturated sterol [1].

Under normal conditions, azole (*N*-substituted imidazole and triazole) antifungal antibiotics cure mycoses by selectively inhibiting the fungal $P450_{14DM}$ at concentrations that are not expected to affect the corresponding host enzyme. They prevent the binding of the natural substrate lanosterol to $P450_{14DM}$ by coordination of the ring nitrogen atom (N3 of imidazole and N4 of triazole) to the sixth coordination position of the iron atom of the enzyme protoporphyrin system [2]. The accumulation of 14α-methylated sterols in azole-treated fungal cells affects membrane structure and functions, resulting in an inhibition of the growth of fungi [3].

The search for better antifungal agents with increased specificity toward fungal enzymes remains a primary target in medicinal chemistry research. Moreover, in the wake of the new regulatory policies, many efforts are currently directed toward the development of enantiomerically pure drugs [4]. With these aims in mind, the azole antifungal agents **1b–h** and **2a–4v** (Fig. 1 and Table 1), structurally related to bifonazole (**1a**) and already investigated by using CoMFA (a 3D-QSAR computational technique) [5], were considered for a new computer-aided drug design study.

*Plenary lecture presented at the Hungarian–German–Italian–Polish Joint Meeting on Medicinal Chemistry, Budapest, Hungary, 2–6 September 2001. Other presentations are published in this issue, pp. 1387–1509.

†Corresponding author

Table 1 Substitution pattern and antimycotic activities of the compounds considered in this study.

Compound	R	R_1	X	Y	MIC (μM/mL) (Observed)[1]	MIC (μM/mL) (Calculated)
1a	H	Ph			1.0	0.87
1b	H	1-pirrolyl			0.26	1.1
1c[2]	H	NO_2			2.2	1.3
1d	CH_3	1-pirrolyl			0.13	0.22
1e[2]	Cl	NO_2			1.0	1.3
1f	CH_3	NO_2			0.50	0.68
1g[2]	Cl	1-pirrolyl			0.46	0.49
1h	H	NH_2			2.5	13
1i	H	Cl			//[3]	//[4]
2a[2]	H	4-Cl	CH	CH	4.0	10
2b	H	2,4-Cl_2	CH	CH	3.6	3.3
2c	H	4-NH_2	CH	CH	2.1	1.5
2d	H	3-(1-pirrolyl)	CH	CH	56	57
2e	H	4-Cl	CH	N	63	47
2f	H	2-Cl	CH	CH	63	4.6
2g	H	3-F	CH	CH	66	56
2h	H	4-OCH_3	CH	N	63	69
2i	H	2-(1-pirrolyl)	CH	CH	7.2	1.7
2j[2]	H	4-NO_2	CH	CH	32	5.6
2k[2]	H	4-OCH_3	CH	CH	8.0	1.8
2l[2]	H	4-Cl	N	CH	32	20
2m	C_2H_5	4-NO_2	CH	CH	7.0	4.0
2n	H	3-Cl	CH	CH	32	27
2o[2]	H	2-F	CH	CH	63	25
2p	H	4-F	CH	CH	16	20
2q	C_2H_5	4-Cl	N	CH	29	23
2r	C_2H_5	4-Cl	CH	N	63	20
3a	H	H			3.1	1.8
3b[2]	CH_3	H			1.0	0.41
3c	Cl	Cl			3.0	0.69
3d[2]	F	Cl			2.0	1.5
3e[2]	H	Cl			0.5	1.7
3f	CH_3	F			1.9	0.61
3g	Cl	F			2.0	1.3
3h[2]	H	F			4.0	3.1
3i[2]	F	H			2.0	1.3
3j	CH_3	Cl			0.89	0.36
3k[2]	F	F			1.0	2.4
4a	Ph	Cl	H		0.46	2.5
4b	Ph	Cl	CH_3		1.0	2.1
4c	Ph	F	H		1.0	4.0
4d	Ph	H	2,4-Cl_2-Bn		22	15
4e	1-naphthyl	H	H		7.9	9.9
4f	Ph	CH_3	CH_3		3.8	2.6
4g	Ph	H	CH_3		4.0	4.5
4h[2]	Ph	F	CH_3		4.0	3.4
4j[2]	1-naphthyl	H	CH_3		27	9.7
4k	H	Cl	CH	CH	0.77	5.2
4l[2]	Me	Cl	CH	CH	3.0	5.6

(*Continued on next page*)

Table 1 (*Continued*)

Compound	R	R_1	X	Y	MIC (μM/mL) (Observed)[1]	MIC (μM/mL) (Calculated)
4m	H	CN	CH	CH	6.3	26
4n[2]	Et	Cl	CH	CH	2.9	14
4o	H	Cl	N	CH	100	20
4p	H	SMe	CH	CH	3.0	4.7
4q[2]	H	CF_3	CH	CH	0.71	4.8
4r	H	NO_2	CH	CH	1.5	2.4
4s	H	1-pirrolyl	CH	CH	0.71	1.6
4t	H	t-But	CH	CH	95	14
4u[2]	H	Ph	N	CH	5.6	1.8
4v[2]	H	Ph	CH	N	100	20

[1]Scaled with respect to compound **1a**.
[2]Compounds forming the test set.
[3]See Table 2.
[4]Value not calculated.

RATIONAL DESIGN AND SYNTHESIS OF NEW DERIVATIVES

Promising results had been already obtained with the CoMFA approach, by the development of a model (COMFA96 hereafter), which successfully explained structure–activity relationships of bifonazole-like inhibitors. Moreover, the alignment method utilized to derive the model gave an insight into a possible binding mode between the inhibitors and the protoporphyrin system of the target enzyme. As a consequence of these findings, following a rational design approach, COMFA96 was applied to predict the inhibitory activities of new antifungal agents **1i** and **5a,b** (Fig. 1 and Table 2) that were then synthesized.

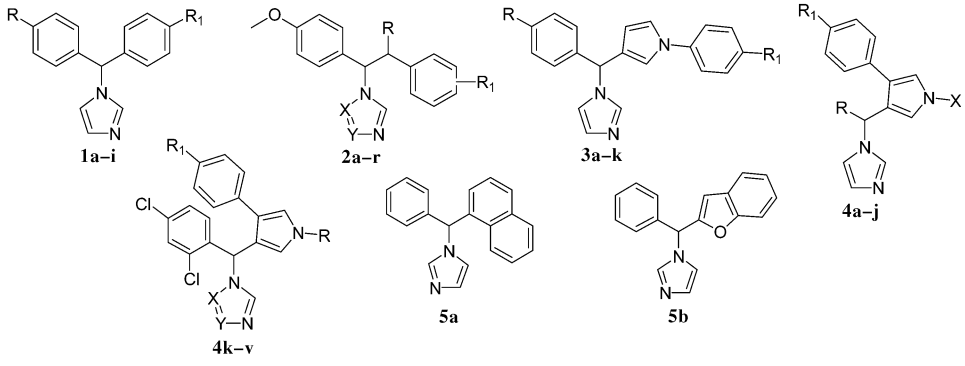

Fig. 1 Antifungal agents considered in this study.

Due to the fact that there is limited information in the literature on the preparation of enantiomers of azole compounds, and only a few examples of enantiopure azole derivatives having the azole moiety directly linked to the stereogenic center have as yet been reported [6], we directed our efforts to the preparation of compounds **1a,i** and **5a,b** in homochiral form for subsequent biological evaluation following the new regulatory guidelines. These derivatives were considered an important synthetic target as the inhibitory activities of their *R*-enantiomers had been predicted by COMFA96 to be comparable with that of (*R*)-**1a** (see Table 2). Notably, all these compounds have been previously synthesized and tested for their antifungal and/or aromatase-inhibiting activity in racemic form [7–9].

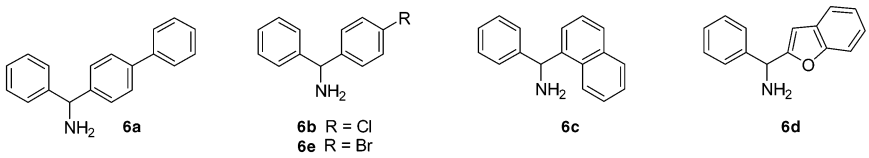

Fig. 2 Amines used for the synthesis of **1a,i** and **5a,b**.

The synthesis of both enantiomers of **1a,i** and **5a,b** started from enantiomerically pure or enriched amines **6a–d** (Fig. 2).

(*R*)- and (*S*)-**6d** were prepared from (*S*)- and (*R*)-1-phenyl-2-propynylamine (**7**) [10] respectively, by heteroannulation with 2-iodophenol (Scheme 1) following a procedure recently described by us for the preparation of the corresponding alcohols [11].

1-Phenyl-2-propynylamine (**7**), attractive synthon for the preparation of a series of bioactive compounds, was kinetically resolved with high stereoselectivity and in good chemical yield using lipase B from *Candida antarctica* (Novozym 435) to provide (*S*)-(**7**) and (*R*)-*N*-(1-phenyl-2-propynyl)acetamide (*R*)-(**8**) (Scheme 2).

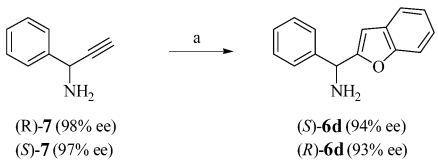

Scheme 1 Reaction conditions: a) 2-iodophenol, $PdCl_2(PPh_3)_2$, CuI, TMG, DMF.

The latter was hydrolyzed to the corresponding (*R*)-(**7**) without loss of enantiomeric purity. (*R*)-**6d** and (*S*)-**6d** were obtained with only a slight decrease in enantiomeric purity (93% and 94% ee, respectively, as determined by enantioselective HPLC) with respect to the starting amine in very good yeld. Both enantiomers of homochiral amines **6b** (>98% ee) and **6c** (80% ee) were prepared according to the literature [12,13]. The knowledge of the absolute configurations [13] of (*S*)-(+)-**6c** and (*R*)-(−)-**6c** allowed to infer the absolute configuration of **6b**, by means of the comparison of their circular dichroism (CD) curves. Finally, (*R*)- and (*S*)-**6a** were obtained in high enantiomeric purity (>98% ee) from (*R*)- and (*S*)-4-bromobenzidrylamine (**6e**) via Suzuki coupling with phenylboronic acid (Scheme 3) and proved to be identical with the compounds obtained through the tedious resolution of the racemic base by means of L-(+)-tartaric acid [14].

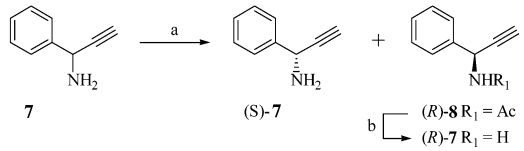

Scheme 2 Reaction conditions: a) CAL, AcOEt, Et_2O; b) HCl.

Elaboration of **6a–d** was carried out through a reaction sequence (Scheme 4) involving *N*-alkylation with bromoacetaldehyde dimethyl acetal to give **9a–d**, followed by *N*-formylation of **9a–d** with butyl formate to afford intermediates **10a–d** as a mixture of rotamers in the ratio 2:1. Finally, ring closure by heating in the presence of ammonium acetate/acetic acid, provided the final compounds **1a** and

5a–c in good chemical yield (60–94%) and with high stereoselectivity (78–>98% ee). The enantiomeric excess was determined by enantioselective HPLC on chiral columns Chiralpak AD (**1a, 5a, 5b**) and Chiralcel OD (**1i**) using multiple detections: UV/CD and polarimetric [15].

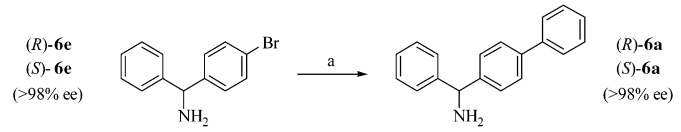

Scheme 3 Reaction conditions: a) phenylboronic acid, $Pd(OAc)_2$, PPh_3, Na_2CO_3, PrOH, H_2O.

The enantiomers of compounds **1a,i** and **5a,b** were tested against *Candida albicans* strains in comparison with the corresponding racemates as well as to fluconazole and amphotericin B as reference standards using the microbroth dilution method [15]. In particular, one laboratory strain of *C. albicans* and two clinical isolates, one of which (L3107 strain) is fluconazole-resistant, were used. The results, expressed as minimal inhibitory concentration (MIC), are reported in Table 2. All the tested

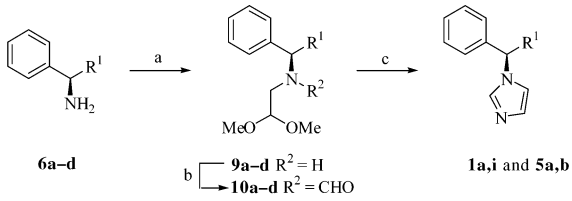

Scheme 4 Reaction conditions: a) $BrCH_2CH(OMe)_2$, K_2CO_3, DMF; b) BuOCHO, reflux; c) $AcONH_4$, AcOH. For simplicity, only the (S)-enantiomers are shown. R^1: **a**, 4-biphenylyl; **b**, 4-chlorophenyl; **c**, 1-naphthalenyl; **d**, 2-benzofuranyl (see also Table 1).

Table 2 *In vitro* antimycotic activity of compounds **1a,i** and **5a,b** against *C. albicans* strains.

Compound	MIC (μg/mL)			
	C. albicans ATCC90028 L3023	*C. albicans* clinical isolate L145	*C. albicans* clinical isolate L3107[a]	COMFA96
(*R*)-**1a**	1	1	>64	1
(*S*)-**1a**	1	1	>64	
(*R,S*)-**1a**	1	1	>64	
(*R*)-**1i**	1	1	32	2
(*S*)-**1i**	1	2	32	
(*R,S*)-**1i**	2	1	64	
(*R*)-**5a**	2	2	32	2
(*S*)-**5a**	1	2	32	
(*R,S*)-**5a**	2	1	8	
(*R*)-**5b**	2	2	16	8
(*S*)-**5b**	2	2	16	
(*R,S*)-**5b**	1	2	32	
fluconazole	0.5	0.5	>64	
amphotericin B	0.5	0.5	1	

[a]Fluconazole-resistant strain.

compounds showed essentially the same antimycotic profile and, quite unexpectedly, in no case was a differential activity between the two enantiomers of each compound observed, even if the activities were similar to those predicted by our previous CoMFA model [5]. This lack of stereoselectivity is not due to racemization of the compounds in the test medium [17], nor necessarily reflects the insensitivity of the putative fungal target (cytochrome P-450-dependent lanosterol 14α-demethylase) to the stereochemistry of the inhibitors, but might be the consequence of other phenomena occurring somewhere in the mechanism of action, from uptake by the cells to inhibition of the fungal target enzyme.

MOLECULAR MODELING

In spite of the above-reported success, COMFA96 recently failed to predict the MIC of a set of new azole antifungal agents of class 4 (**4k–4v**), synthesized after the derivation of the model, as clearly indicated by the low value computed for the predictive correlation coefficient ($r^2 = 0.52$). These unexpected results pointed out the need for a sounder interaction model, with better possibilities for description and prediction, consequently, we resorted to another QSAR approach.

In this study, the pseudoreceptor modeling technique [17,18] was applied with the primary goal to explain and predict the activity of general azole *C. albicans* $P450_{14DM}$ inhibitors, including those compounds whose activity was not rationalized by COMFA96 (**4k–4v**), in order to bring up to date our previous interaction model [5]. Even though the biological evaluation of almost all the compounds had been carried out using racemic mixtures, the *R*-enantiomer of bifonazole was arbitrarily modeled here and all the other inhibitors were constructed according to this choice, as already done in the case of COMFA96. The *S*-enantiomers of bifonazole (**1a**), **1i**, and **5a,b** were excluded from the construction of the pseudoreceptor due to their small number with respect to the remainder of the compounds and poor structural diversity. Only compound (*S*)-**1a** was included in the test set to evaluate the preference of the final model for one enantiomeric series of inhibitors relative to the other.

The methodology of pseudoreceptor modeling is well established and has been recently reviewed in a detailed manner [18]. In this application, the three-dimensional coordinates of the ligand molecules, superimposed in their bioactive conformation (according to our previous CoMFA study results), were used as the ligand alignment [5], while the experimental free energies of ligand binding were calculated according to a methodology reported in the literature [19]. The whole set of compounds **1–4** was considered to generate and validate the model, selecting 36 compounds as the training set (**1a**, **1b**, **1d**, **1f**, **1h**, **2b**, **2c**, **2d**, **2e**, **2g**, **2h**, **2i**, **2m**, **2n**, **2p**, **2q**, **2r**, **3a**, **3c**, **3f**, **3g**, **3j**, **4a**, **4b**, **4c**, **4d**, **4e**, **4f**, **4g**, **4k**, **4m**, **4o**, **4p**, **4r**, **4s**, **4t**). The two steps corresponding to identification of the receptor nucleation sites and construction of the pseudoreceptor were accomplished accordingly to the PrGen default methodology [17]: vectors were associated to any atom of ligand molecules constituting the training set and analyzed for clustering. The N-3 nitrogen atom of the azole ring, the centroid of the ubiquitous phenyl ring on the chiral carbon atom (interaction site relevant for inhibitor-enzyme recognition) and the 4-substituent on the same ring (interaction site responsible for ligand selectivity) resulted to be regions with a high vector density. The large aromatic moiety (a biphenyl group in the case of **1a**), on the contrary, seemed a spatial zone with a lower probability for finding important interaction sites, as a low clustering was observed. Notably, some authors consider this long chain only important to improve the physicochemical properties and the pharmacodynamic and pharmacokynetic profiles of molecules [20].

Residues crucial for binding have not been experimentally detected in the case of the inhibitors of $P450_{14DM}$, with the exception of the heme moiety. Consequently, to generate the pseudoreceptor model, a Fe(III)-heme was placed as a coordination bond acceptor at the N-3 nitrogen atom of azole ring. The vectors associated by PrGen to the 4-methylphenyl group of **1d** were saturated by lipophilic interactions with one histidine, one lysine, one tryptophane and two phenylalanine [21], while one threonine residue was located with the OH group on the side chain directed perpendicularly to the azole ring toward it [20]. Finally, one phenylalanine and one tyrosine were placed below the large aromatic

moiety, one serine above it, and three more residues (serine, proline, and threonine) surrounded at the side of the hydrogen atoms.

A receptor equilibration was performed allowing translation, rotation, and torsional variations of the receptor residues, whereas the ligands were kept fixed in their original arrangement. Subsequently, the ligands were allowed to relax within the binding pocket. Repeating these two steps several times, the so-called ligand equilibration yielded a pseudoreceptor model with a good correlation ($r^2 = 0.85$) between experimentally detected and calculated activity data (see Table 1) and a root mean square (rms) value of 0.56 kcal/mol.

A test set of 23 ligands [(*S*)-**1a**, **1c**, **1e**, **1g**, **2a**, **2f**, **2j**, **2k**, **2l**, **2o**, **3b**, **3d**, **3e**, **3h**, **3i**, **3k**, **4h**, **4j**, **4l**, **4n**, **4q**, **4u**, **4v**] was then introduced within the binding pocket. Only in the case of (*S*)-**1a**, a Monte Carlo simulation was performed to determine its orientation inside the catalytic site, while the other compounds were superimposed by a rigid fit onto the compounds of the training set and submitted to a simple relaxation by minimization of the binding free energy. The procedure yielded an rms deviation for the predicted free energies of binding of 0.65 kcal/mol (excluding (*S*)-**1a**) corresponding to a factor of about 2.6 in the activity values (see Table 1). Notably, (*S*)-**1a** showed a peculiar orientation in the pseudoreceptor cavity with respect to the other compounds (in Fig. 3, the docking of this compound and that of its epimer (*R*)-**1a** inside the final model are depicted). This mapping gave a worse activity correlation with respect to the *R*-enantiomer (12 predicted vs. 1.0 experimental), which was expected as only one enantiomeric series of compounds was used to build the pseudoreceptor, due to a worse complementarity of the chemical groups of the ligand with respect to the residues of the enzyme surrogate. It has to be noted however that, although no differential activity between the two enantiomers of compound **1a** should have been predicted, the present computational analysis suggested the possible binding mode of the two enatiomers of bifonazole into the catalytic site of *C. albicans* $P450_{14DM}$, as depicted in Fig. 3.

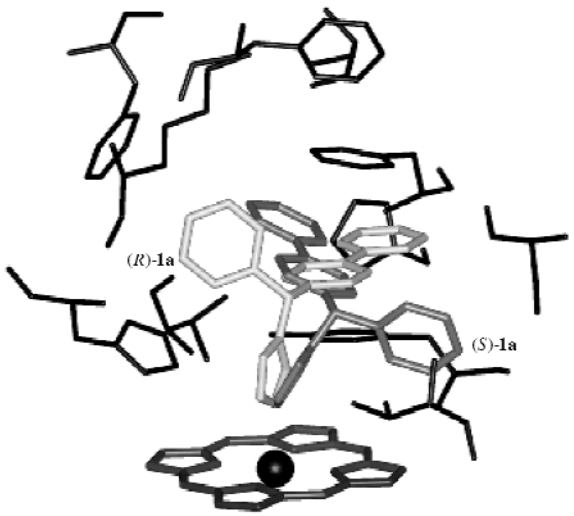

Fig. 3 Docking of (*S*)-**1a** and (*R*)-**1a** inside the final pseudoreceptor model.

The final pseudoreceptor model is composed of 12 amino acid residues in addition to the heme moiety. The key binding functions are taken by the Fe(III) ion, acting as coordination bond acceptor for the nitrogen atom of imidazole and triazole (all the ligands coordinate the sixth position of the iron ion with the N-3 or N-4 nitrogen atom of the azole ring), and one tyrosine residue stabilizing the most active

compounds via a π-π stacking interaction with one of the aromatic rings (the pirrole in the case of **1d**). Furthermore, five aromatic residues, three phenylalanine, one tryptophane and one hystidine, wrap the phenyl locus (left side in Fig. 3). A threonine is placed above the porphyrin plane, in a very similar way with respect to Thr 311 of the natural enzyme model [20,21]. One lysine acts simultaneously as hydrogen bond acceptor (via main-chain carbonyl oxygen) and donor (via main-chain amino group and terminal side-chain amino group) with other amino acid residues, contributing to the stability of the complex and completing the necessary requirements of this pseudoreceptor model. The inhibitors interact, in a nonspecific manner, with the active-site chamber dome residues (mainly lipophilic) that constituted the ceiling above the porphyrin plane, and these results appear in agreement with recent findings on a $P450_{14DM}$ enzyme from *Mycobacterium tuberculosis* [22].

The promising results obtained with the pseudoreceptor modeling approach reported here demonstrate its validity in bridging structure-based receptor fitting and property-based receptor mapping methodologies to study and propose macromolecular binding sites and predict their interactions with bioactive conformers of the ligands. The final pseudoreceptor model, in fact, seemed able to correctly estimate and predict the anti-*Candida* activity of the studied compounds.

REFERENCES AND NOTES

1. M. Akhtar and J. N. Wright. *Nat. Prod. Rep.* **8**, 527–551 (1991).
2. C. A. Hitchcock, K. Dickinson, S. B. Brown, E. G. V. Evans, D. J. Adams. *Biochem. J.* **266**, 475–480 (1990).
3. P. L. Yeagle, R. B. Martin, A. K. Lala, H. K. Lin, K. Blok. *Proc. Natl. Acad. Sci. USA* **74**, 4924–4926 (1977).
4. R. McCague and G. Casy. In *Progress in Medicinal Chemistry,* Vol. 34, G. P. Ellis and D. K. Luscombe (Eds.), pp. 203–261, Elsevier, Amsterdam (1997).
5. A. Tafi, J. Anastassopoulou, T. Theophanides, M. Botta, F. Corelli, M. Artico, R. Costi, R. Di Santo, S. Massa, R. Ragno. *J. Med. Chem.* **39**, 1227–1235 (1996).
6. (a) F. Corelli, V. Summa, A. Brogi, E. Monteagudo, M. Botta. *J. Org. Chem.* **60**, 2008–2015 (1995); (b) M. Botta, V. Summa, G. Trapassi, E. Monteagudo, F. Corelli. *Tetrahedron: Asymmetry* **5**, 181–184 (1994).
7. **1i**: C. D. Jones, M. A. Winter, K. S. Hirsch, N. Stamm, H. M. Taylor, H. E. Holden, J. D. Davenport, E. V. Krumkalns, R. G. Suhr. *J. Med. Chem.* **33**, 416–429 (1990).
8. **5a**: M. Artico, G. Stefancich, R. Silvestri, S. Massa, G. Apuzzo, M. Artico, G. Simonetti. *Eur. J. Med. Chem.* **27**, 693–699 (1992).
9. **5b**: (a) L. Banting. In *Progress in Medicinal Chemistry*, Vol. 33, G. P. Ellis and D. K. Luscombe (Eds.), pp. 147–184, Elsevier, Amsterdam (1996); (b) L. Riviera, M. G. Bellotti, V. Pestellini, D. Giannotti, A. Giolitti, N. Fantò. *Chemioterapia* **6**, 272–276 (1987); (c) V. Pestellini, D. Giannotti, A. Giolitti, N. Fantò, L. Riviera, M. G. Bellotti. *Chemioterapia* **6**, 269–271 (1987).
10. F. Messina, M. Botta, F. Corelli, M. P. Schneider, F. Fazio. *J. Org. Chem.* **64**, 3767–3769 (1999).
11. M. Botta, V. Summa, F. Corelli, G. Di Pietro, P. Lombardi. *Tetrahedron: Asymmetry* **7**, 1263–1266 (1996).
12. **6b**: G. R. Clemo, C. Gardner, R. Raper. *J. Chem. Soc.* 1958–1960 (1939).
13. **6c**: R. Annunziata, M. Cinquini, F. Cozzi. *J. Chem. Soc., Perkin Trans. 1*, 339–343 (1982).
14. S. K. Hsu, C. K. Ingold, C. L. Wilson. *J. Chem. Soc., Perkin Trans. 2*, 1778–1785 (1935).
15. M. Botta, F. Corelli, F. Gasparrini, F. Messina, C. Mugnaini. *J. Org. Chem.* **65**, 4736–4739 (2000).
16. Samples dissolved in DMSO/water (1/9, v/v) at pH 7 (phosphate buffer), and stored at 35 °C for 24 h did not show any decrease of the ee value.
17. P. Zbinden, M. Dobler, G. Folkers, A. Vedani. *Quant. Struct–Act. Relat.* **17**, 122–126 (1998).
18. M. Gurrath, G. Müller, H. D. Höltje. In *3D QSAR in Drug Design*, H. Kubinyi, G. Folkers, Y. C. Martin (Eds.), pp. 135–157, Kluwer, Dordrecht (1998).

19. A. Bassoli, L. Merlini, G. Morini, A. Vedani. *J. Chem. Soc., Perkin Trans. 2*, 1449–1454 (1998)
20. H. Ji, W. Zhang, Y. Zhou, M. Zhang, J. Zhu, Y. Song, J. Lü, J. Zhu. *J. Med. Chem* **43**, 2493–2505 (2000).
21. P. E. Boscott and G. H. Grant. *J. Mol. Graph.* **12**, 185–192 (1994).
22. L. M. Podust, T. L. Poulos, M. R. Waterman. *Proc. Natl. Acad. Sci.* **98**, 3068–3073 (2001).